Planetary and Space Science 102 (2014) 164–170

Contents lists available at ScienceDirect

Planetary and Space Science

journal homepage: www.elsevier.com/locate/pss

The meteoroid environment and impacts on Phobos

Apostolos A. Christou [a,*], Jürgen Oberst [b,c], Valery Lupovka [d], Vasily Dmitriev [d], Maria Gritsevich [g,f,e]

[a] Armagh Observatory, College Hill, Armagh BT61 9DG, Northern Ireland, UK
[b] German Aerospace Centre, Institute of Planetary Research, Rutherfordstrasse 2, D-12489 Berlin, Germany
[c] Technische Universität Berlin, Institute for Geodesy and Geoinformation Science, Planetary Geodesy, Strasse des 17. Juni 135, 10623 Berlin, Germany
[d] Moscow State University for Geodesy and Cartography, Extraterrestrial Laboratory, 4, Gorokchovsky pereulok, 105064 Moscow, Russia
[e] Russian Academy of Sciences, Dorodnicyn Computer Centre, Department of Computational Physics, Vavilova ul. 40, 119333 Moscow, Russia
[f] Ural Federal University, Institute of Physics and Technology, Department of Physical Methods and Devices for Quality Control, Mira ul. 19, 620002 Ekaterinburg, Russia
[g] Finnish Geodetic Institute, Department of Remote Sensing and Photogrammetry, Geodeetinrinne 2, P.O. Box 15, FI-02431 Masala, Finland

ARTICLE INFO

Article history:
Received 19 February 2013
Received in revised form
11 July 2013
Accepted 26 July 2013
Available online 22 August 2013

Keywords:
Meteoroids
Phobos
Impact cratering
Comets
Asteroids

ABSTRACT

We review current knowledge of the flux of meteoroids on Phobos, a key to interpreting its cratering record and understanding the origin of the Martian satellite system. Past observational attempts to estimate the flux of small (mm to cm) meteoroids as meteors in the Martian atmosphere highlight the need for customised instrumentation onboard future missions bound for Mars. The temporal distribution of cometary meteoroid streams as predicted by recent work is non-uniform; we advocate emplacing seismic stations on Phobos or cameras optimised to monitor the Martian atmosphere for meteors as a means to elucidate this and other features of the meteoroid population. We construct a model of the sporadic flux of metre-sized or larger meteoroids and use it to predict a leading/trailing ratio in crater density of ~ 4 if crater production by asteroidal meteoroids dominates over that by cometary ones. It is found that the observed distribution of craters ≥ 100 m as determined from spacecraft images is consistent with a 50/50 contribution from the two meteoroid populations in our model. A need for more complete models of the meteoroid flux is identified. Finally, the prospects for new observational constraints on the meteoroid environment are reviewed.

1. Introduction

As with every other body in the solar system, the Martian system is subject to a continuous influx of meteoroids ranging in size from under a μm to several km. Their effect on the Martian atmosphere is to produce ionisation layers (Pätzold et al., 2005) and meteors (Adolfsson et al., 1996) with the larger ones reaching the Martian surface and creating impact craters, crater clusters or meteorites (Flynn and McKay, 1989; Popova et al., 2003; Chappelow and Sharpton, 2006). Impacts of "large" (metre-sized or larger) meteoroids on the airless surface of Phobos is the primary process for producing the craters seen in spacecraft images. In addition, seismic shaking and the production of ejecta contribute to the displacement and transport of surface material. On the other hand, impacts by "small" (decimetre or smaller) meteoroids can launch ejecta in circum-martian space, contributing to the dust environment in the orbital vicinity of this moon (e.g. Krivov and Hamilton, 1997). Consequently, as can be read in the relevant chapters of this volume, an independent determination of the meteoroid flux is needed to compare with models of the production rate of craters and boulders on Phobos, the impact flux on Mars itself now and in the past as well as the dust torus that is postulated by several studies.

A study of the Phobos meteoroid environment also has value in itself. It represents an opportunity to learn more about the population of meteoroids which do not intersect the Earth's orbit. The physical properties of meteoroids causing meteors in the Earth's atmosphere have been studied theoretically in a number of works (Lebedinets, 1987; Babadzhanov, 1994; Kikwaya et al., 2006). According to the classical physical theory of meteors, these are considered to be solid bodies similar to meteorites of stony/iron composition with bulk densities ranging from 3.5 g cm^{-3} to 7.7 g cm^{-3} (Levin, 1956). Lebedinets (1987) and Babadzhanov (1994) obtained an average bulk density of 3.3 g cm^{-3} with values for individual cases in the range from 0.1 g cm^{-3} to 8.0 g cm^{-3}. Bellot Rubio et al. (2002) gave even lower estimates ranging from 0.1 g cm^{-3} to 4.5 g cm^{-3}. In contrast, a wide range of the laboratory measurements for meteorites, micrometeorites and interplanetary dust particles did not confirm such a low limit for the bulk

* Corresponding author. Tel./fax: +44 2837 522928/+ 44 2837 527174.
E-mail addresses: aac@arm.ac.uk, aac@star.arm.ac.uk (A.A. Christou), juergen.oberst@dlr.de (J. Oberst), v.lupovka@miigaik.ru (V. Lupovka), v.dmitriev@miigaik.ru (V. Dmitriev), gritsevich@list.ru (M. Gritsevich).

0032-0633/$ - see front matter © 2013 Elsevier Ltd. All rights reserved.
http://dx.doi.org/10.1016/j.pss.2013.07.012

density. A selection effect may be at work here since fragile, low density material is likely to ablate and consume itself high in the Earth's atmosphere rather than land as a meteorite. The same is true for the Martian atmosphere (Christou and Beurle, 1999; McAuliffe, 2006) but not for airless Phobos where such objects would impact directly onto the surface.

This work is concerned with the meteoroid environment and impact effects at Phobos, particularly crater production. In the section that follows we review past attempts to constrain the meteoroid flux in the Martian system while in Section 3 we consider the particular question of the existence and detectability of meteoroid streams. In Section 4 we present a model of the "sporadic" (i.e. non-stream) flux of large meteoroids at Phobos. This is used to predict relative crater abundances over its surface through the procedure described in Section 5. Section 6 describes the results of this model and a comparison with observationally determined crater counts from *in situ* spacecraft data. Finally, Section 7 contains our main conclusions and outlines prospects for future development in the field.

2. Observations to-date

No direct *in situ* measurements of the meteoroid flux at Mars exist to-date. Since meteoroids obey a size distribution, the flux of particles larger than a few tens of microns across is too low to be picked up by contemporary instrumentation for dust detection *in situ*. Rather, such particles can be detected as meteors in the Martian atmosphere (Adolfsson et al., 1996; McAuliffe and Christou, 2006). Adolfsson et al. (1996) estimated the flux of meteoroids producing so-called "photographic" meteors – i.e. in the absolute visual magnitude range -1 m to $+4$ m – at Mars to be 50% of that at the Earth. Domokos et al. (2007) concluded that the negative result of their meteor search in nighttime images taken by the MER rovers, which they translated into an upper flux limit of 4.4×10^{-6} km^{-2} h^{-1} for a mass lower limit of 4 g, was broadly consistent with the Adolfsson et al. prediction of $\sim4\times10^{-7}$ km^{-2} h^{-1} derived by their scaling of the Earth flux according to the Grün et al. (1985) model. No imaging system suitable for the routine detection of meteors in the Martian atmosphere has yet flown but many of the key technologies are now available (Oberst et al., 2011). A detection of a meteor associated with a known Jupiter-family comet by the dual-eye Pancam imager onboard the Spirit rover on Mars was claimed by Selsis et al. (2005). Later work by Domokos et al. (2007) quantified the effects of cosmic ray hits (CRHs) on the Spirit Pancam as part of a dedicated meteor search and placed the 2005 detection in doubt.

3. Streams

Many cometary meteoroids remain close to the orbit of the parent comet for up to $\sim10^5$ yr forming dense *streams* (McIntosh, 1991). These create meteor showers in the atmospheres of the Earth, where they dominate the bright ($+0$ m to -4 m) meteor flux (Hughes, 1987; Atreya and Christou, 2009). The majority of observational and theoretical work to-date concerns this class of meteoroids. Their orbits retain a memory of their birth, with the result that, if observed and recorded, they can be associated with their specific comet of origin.

In addition, the high particle density within *trails*, which results in short-lived outbursts (of duration a few hour) in meteor activity when these trails encounter the Earth's atmosphere (e.g. McNaught and Asher, 1999), produce a proportionate increase in meteoroid flux on the surfaces of airless bodies. For example, the flux corresponding to a Leonid-type meteor storm translates into 400 meteoroids ≥1 mm in size impacting the surface of a body with the dimensions of Phobos every hour (Christou and Beurle, 1999) exceeding the sporadic flux of same-sized objects at the Earth by ~4 orders of magnitude.

In the absence of observations, arguments for the existence of Mars-intersecting meteoroid streams have been primarily based on orbital geometry considerations (Terentjeva, 1993; Christou and Beurle, 1999; Treiman and Treiman, 2000; Larson, 2001; Selsis et al., 2004; Neslusan, 2005; Jenniskens, 2006). Christou (2010) re-examined the problem of meteor shower parenthood in light of the tendency for strong meteor showers at the Earth to be associated with certain types of comets (e.g. Halley-type) rather than others. He identified 19 Intermediate Long Period (ILPCs) and Halley Type Comets (HTCs) that are potentially responsible for meteor showers at Mars. In addition, that author found that most of the meteoroid streams associated with Encke-type comets and responsible for shower activity at the Earth are likely to also intersect the orbit of Mars. Expected characteristics of these showers such as speed and radiant location – but not their intensity or particle population properties – can be determined in a straightforward way from the planet-approaching geometry and are illustrated in Fig. 1. Filled circles correspond to Halley-Type (HTCs) and Intermediate Long Period Comets (ILPCs) while open circles correspond to Encke-Type Comets (ETCs). The size of the circle is proportional to the impact speed in the Martian atmosphere while the colour indicates either a radiant near the Sun (bright red), along the terminator (dark red) or in the anti-Sun direction (black). The location corresponding to $L_S=0^\circ$ is indicated by the grey arrow. It is noted that the temporal distribution of these putative streams is non-uniform with twice as many stream encounters occurring during the period $180^\circ \lesssim L_S \lesssim 360^\circ$.

Christou and Vaubaillon (2011) refined the results of Christou by simulating numerically these meteoroid streams. They found

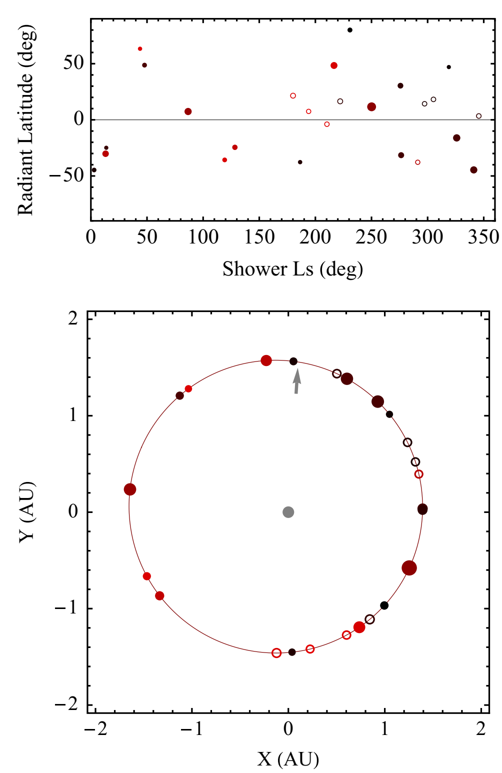

Fig. 1. Top: Areocentric latitudes referenced to the Martian equator as a function of L_S for the radiants of the shower candidates given in Christou (2010). Bottom: Location of the shower candidates along the Martian orbit. See the text for details. (For interpretation of the references to colour in the main text the reader is referred to the web version of this article.)

that in 9 cases, a significant fraction of test meteoroids encounter the orbit of Mars and can produce annually recurring showers, the intensity of which remains to be calibrated through observations.

Potential meteoroid flux enhancements will occur as the Martian system passes through a stream. This may be detected by e.g. emplacing seismic stations on Phobos as was done previously for the Moon (Oberst and Nakamura, 1991) or through the meteors produced in the Martian atmosphere (Adolfsson et al., 1996; Christou and Beurle, 1999; Christou et al., 2012). Their effect, if any, on the density and distribution of circum-martian dust is another open question.

4. A model of the sporadic meteoroid flux at Phobos

Asteroidal and cometary meteoroids that have suffered significant dynamical evolution after ejection form the *sporadic* continuum (or sporadic background). Recently, Wiegert et al. (2009) produced a self-consistent model of the sporadic meteoroid complex at the orbit of the Earth and concluded that (a) most sporadic meteoroids are of cometary origin and (b) the bulk of the sporadic flux is provided by only a fraction of the comet population. No similar model exists for Mars, partly because there is no data on meteoroid flux (e.g. from meteor observations) that such a model can be fitted to. It can, however, be fitted to Phobos crater abundances. In what follows we describe a relatively simple model of the flux of crater-producing meteoroids at Phobos that we use to predict the relative density of craters over different areas of its surface. The model is simple in that it assumes that the meteoroid flux is solely due to the known Mars-approaching asteroids and comets serving as the parent bodies. It does not take into account the orbital evolution of either the parent bodies or their meteoroids. Although the model encompasses, by definition, both the stream and sporadic flux we assume, as is the case for the Earth (Jones and Brown, 1993; Brown et al., 2008), that the meteoroid flux within streams is a minor contributor to the overall flux. Finally, we note that the crater-producing meteoroids we consider here are metre-sized or larger as opposed to the sub-mm to cm meteoroids considered in the work by Wiegert et al. (2009). They are, however, generally smaller than the objects considered in studies of the impact flux and crater production on the Moon (Gallant et al., 2009; Ito and Malhotra, 2010; Le Feuvre and Wieczorewk, 2011). Non-gravitational forces such as Poynting–Robertson drag as included in the work by Wiegert et al. will be ineffective in modifying the orbits of the meteoroids considered in the present work. Instead, the Yarkovsky effect, not included in our model, will likely result in significant orbital changes over time (Farinella et al., 1998).

4.1. The Cometary component

From a database of 1037 periodic comets within JPL's HORIZONS service (http://ssd.jpl.nasa.gov/?horizons) we found 137 comets in orbits that approach Mars' orbit to within 0.15 AU. Of those, 54 are Jupiter Family Comets (JFCs) and the remainder are Long Period Comets (LPCs). Both types have been included as they are thought to contribute to different components of the sporadic flux at the Earth. The meteoroid flux for each of these comets at Mars was calculated using the following assumptions:

1. The orbits of the comets change very slowly over time; the theoretical stream radiant positions are therefore fixed.
2. The density of meteoroid orbits in the stream tube is distributed symmetrically with respect to the parent comet orbit, and maximum flux occurs at the comet orbit.
3. Meteoroids are uniformly distributed along the stream orbit, and their distribution does not depend on the position of the parent comet.

Specifically, the cumulative particle flux is modelled as an exponentially decaying function of the distance from the stream centre (Dmitriev et al., 2012a,b).

4.2. The Asteroidal component

Asteroids on Mars-approaching orbits are another potentially important contributor to the Phobos meteoroid environment due to Mars' proximity to the asteroid belt. Using HORIZONS, we identified 5957 asteroids in orbits that approach Mars' orbit to within 0.1 AU. This sample is composed of Apollo and Amor group asteroids, as well as inner main belt members. Modelling of asteroid impact probability was performed using Opik's (1976) method. Formulas from Chesley et al. (2002) were used in order to convert asteroid magnitudes into diameters and masses. The number of asteroids with $H > 18$ suffers from significant observational bias; this was estimated from the distribution of brighter asteroids by extrapolating the Hartmann function (Ivanov et al., 2002) applicable to this latter population.

5. Model of crater production and distribution

For cometary impactors, the cumulative impactor flux ρ was calculated for 60 days before and 60 days after the orbit-crossing point with a time step of one day. The number of potential impacts during this time interval is then

$$N = S_{\mathrm{Phob}} \int_{t_0}^{t_1} \rho(r)\, dt \tag{1}$$

where t_0 and t_1 correspond to the boundaries of the aforementioned 120-day period, S_{Phob} being the surface area of Phobos' disk. For asteroids the probability used for the random generation of impacts was calculated after Opik (1976):

$$p = \frac{f_S^2 (U^2 + 0.625 e_0^2 + \sin^2 i_0)}{2\pi(\sin^2 i + \sin^2 i_0)^{1/2} (U_x^2 + 0.5 e_0^2)^{1/2}} \tag{2}$$

where $f = L/\pi$ with L given by the expression

$$\cos L = \begin{cases} \dfrac{a(1-e) - s' - (1-e_0^2)}{(a(1-e) - s')e_0} & \text{if } a > 1, \\ \dfrac{(1-e_0^2) - s' - a(1+e)}{(a(1+e) + s')e_0} & \text{if } a < 1 \end{cases} \tag{3}$$

where $s' = (2/3)s$, $s^2 = q^2(1 - 2m/qU^2)$ and a is the orbital heliocentric semimajor axis of the impactor in units of that of Mars. Impact directions and velocities were calculated in a Phobos-centric, Phobos-fixed coordinate system. The velocity V of the impactor relative to Phobos is given by

$$V = V_{impactor} - V_{Mars} - V_{Phobos} \tag{4}$$

where $V_{impactor}$ and V_{Mars} are the inertial heliocentric velocities of the comet/asteroid and Mars respectively and V_{Phobos} is that moon's orbital velocity relative to Mars. Applying a uniform random-event generator on the disk perpendicular to the arrival velocity vector (Press et al., 2007) followed by orthographic projection onto a sphere produces the impact location of meteoroids in the inertial frame. These are then transformed into a Phobos-fixed coordinate system using the IAU-recommended rotation model for that moon (Archinal et al., 2009). At the same time, the effect of meteoroid screening by Mars is calculated and – for the slower asteroidal impactors only – the effect of Mars' gravitational attraction is taken into account. The crater size is estimated using the formula by (Bottke et al., 2000):

$$D_c = 1.25(M/\rho)^{1/3}(1.61gd/V_n^2)^{-\beta} \quad (5)$$

where D_c is the crater diameter, M the meteoroid mass, d the meteoroid diameter, g and ρ the gravity acceleration and density at the Phobos surface respectively, V_n the component of the impact velocity that is normal to the Phobos surface and β an experimentally determined constant. The values assumed in this work are: $g = 5.1 \times 10^{-3}$ m s^{-2} and $\rho = 1900$ kg m^{-3}. For β we used the value 0.22 for competent rock or saturated soil from Richardson et al. (2005). The meteoroid diameter is calculated assuming a density of 1200 kg m^{-3} for the cometary case and 2000 kg m^{-3} for the asteroidal one.

6. Results of the sporadic flux model

The results of the model described in Section 4 for both asteroidal and cometary sources were used by the procedure of Section 5 to generate expected relative densities of craters ≥ 100 m in size. These are shown as percentages of the total for the entire surface of Phobos in columns 2–5 of Table 1. Column 6 shows observed relative crater densities on Phobos (see paper by Kharachevtseva et al., 2014) for a completeness diameter limit of 100 m. In what follows we discuss some features observed in the resulting model distributions and compare it with the observed crater densities.

A potential consequence of Phobos' proximity to Mars is a decrease of the impactor flux on the Mars-facing hemisphere of Phobos due to screening by the planet. In our model such a feature exists at the levels of 11% and 2% for the model cometary and asteroidal particles respectively. The difference is likely due to the lower degree of gravitational focusing for the faster-moving cometary particles (see also later discussion on velocity). Also, both northern and southern hemispheres of Phobos are expected to receive the same number of impacts to within 10%.

Interestingly, cometary meteoroids in our model – mainly those from Jupiter-family comets – appear to produce 30% more craters near the equator than near the poles while this trend is reversed for asteroidal meteoroids. The cause of this feature is not immediately obvious since the typical orbital inclinations for the two populations are similar. We believe that a partial explanation may be found in the perihelion distance distributions of the model impactors. Fig. 2 shows these distributions with the perihelion and aphelion distances of Mars indicated by the red bars. Asteroidal and JFC perihelia mainly occur near Mars' distance from the sun. In the case of the highly eccentric JFC orbits, the heliocentric velocity at pericentre is high enough that the velocity relative to Mars is dominated by the ecliptic component. For the asteroidal case however, perihelic velocities of these low-to-moderate eccentricity orbits are similar to the orbital velocity of Mars and the small – in absolute terms – vertical component of the relative velocity becomes significant compared to the ecliptic component. Consequently, asteroidal impactors will appear to approach Mars from high ecliptic latitudes.

Irrespective of the cause of the feature in the model population, there is no clear evidence for it in the observed crater abundances. A higher – by 25% – crater abundance is observed near the South pole relative to the equatorial region but not in the North. Its origin is not clear but may be related to the presence of large craters such as Stickney rather than e.g. a higher proportion of asteroidal impactors on Phobos.

Probably the most significant feature in our model is the difference between the number of model craters on the eastern and western hemispheres of Phobos. These correspond to the regions of its surface that trail and lead respectively in Phobos' motion around Mars; we will also make use of the notation "leading" and trailing" in what follows. The number of cometary meteoroids is 5% larger on the western hemisphere but for asteroidal meteoroids this difference amounts to 45%. In fact, as Table 1 shows, Phobos' leading quadrant – in other words, the centre half of its western hemisphere – should receive four times as many asteroidal impacts as its trailing quadrant.

A clue as to the cause of this asymmetry may be found in the velocity distribution of the impactors (Fig. 3). The majority of cometary impacts occur at velocities ranging from 20 to 50 km s^{-1} for the Long Period population and 15 to 30 km s^{-1} for the Jupiter Family population. On the other hand, asteroidal impacts occur at velocities between 2 and 5 km s^{-1}, comparable to the orbital velocity of Phobos around Mars (2.1 km s^{-1}) as well as the escape velocity at Phobos' distance from Mars (~ 3 km s^{-1}).

Under the circumstances applicable to asteroidal impacts, a satellite in a synchronous lock with its primary will receive a significantly higher flux of impactors on its leading side than on the trailing side (see Kawamura et al., 2011, and references therein). Following Gallant et al. (2009) (see also Zahnle et al., 2001) this asymmetry can be expressed as

$$\Gamma(\beta) = \overline{\Gamma}(1 + \alpha \cos \beta)^g \quad (6)$$

where β is the elongation angle from the apex of Phobos' orbital motion around Mars and $\overline{\Gamma}$ represents the crater density at $\beta = 90^\circ$. The quantity α is given by the ratio between v_{orb}, Phobos' orbital velocity, and v_{imp}, the velocity of the projectile with hyperbolic velocity v_∞ at the areocentric distance of that moon, in other words $\alpha = v_{orb}/\sqrt{2v_{orb}^2 + v_\infty^2}$. The exponent g depends on the size distribution of the impactors. Here we adopt the value

Table 1
Statistics of model and observed meteoroid impact craters on Phobos.

Location on Phobos	Long Period comets	Jupiter Family comets	All comets	Asteroids	Observed crater abundance
Sub-Mars ($-45^\circ < \lambda < 45^\circ$)	23.1 ± 1.3	21.7 ± 1.3	21.4 ± 1.3	22.5 ± 1.3	26.0
Trailing ($45^\circ < \lambda < 135^\circ$)	23.4 ± 1.3	23.9 ± 1.4	24.2 ± 1.4	10.8 ± 0.9	15.9
Anti-Mars ($135^\circ < \lambda < 225^\circ$)	26.1 ± 1.4	26.7 ± 1.4	26.6 ± 1.4	24.4 ± 1.4	24.9
Leading ($225^\circ < \lambda < 315^\circ$)	27.4 ± 1.5	27.7 ± 1.5	27.8 ± 1.5	42.3 ± 1.8	33.2
North polar ($\phi > 30^\circ$)	25.4 ± 1.4	19.5 ± 1.2	19.5 ± 1.2	28.7 ± 1.5	22.6
South polar ($\phi < -30^\circ$)	25.3 ± 1.4	21.7 ± 1.3	21.7 ± 1.3	26.1 ± 1.4	30.1
South equatorial ($-30^\circ < \phi < 0^\circ$)	24.2 ± 1.4	28.9 ± 1.5	29.9 ± 1.5	23.3 ± 1.3	24.9
North equatorial ($0^\circ < \phi < 30^\circ$)	25.2 ± 1.4	29.0 ± 1.5	28.9 ± 1.5	21.9 ± 1.3	22.4
Northern hemisphere	50.6 ± 2.0	48.5 ± 1.9	48.4 ± 1.9	50.6 ± 2.0	47.3
Southern hemisphere	49.4 ± 1.9	51.5 ± 2.0	51.6 ± 1.9	49.4 ± 1.9	52.7
Western hemisphere	52.7 ± 2.0	52.7 ± 2.0	52.7 ± 2.0	72.5 ± 2.5	57.3
Eastern hemisphere	47.4 ± 1.9	47.3 ± 1.9	47.3 ± 1.9	27.5 ± 1.5	42.7

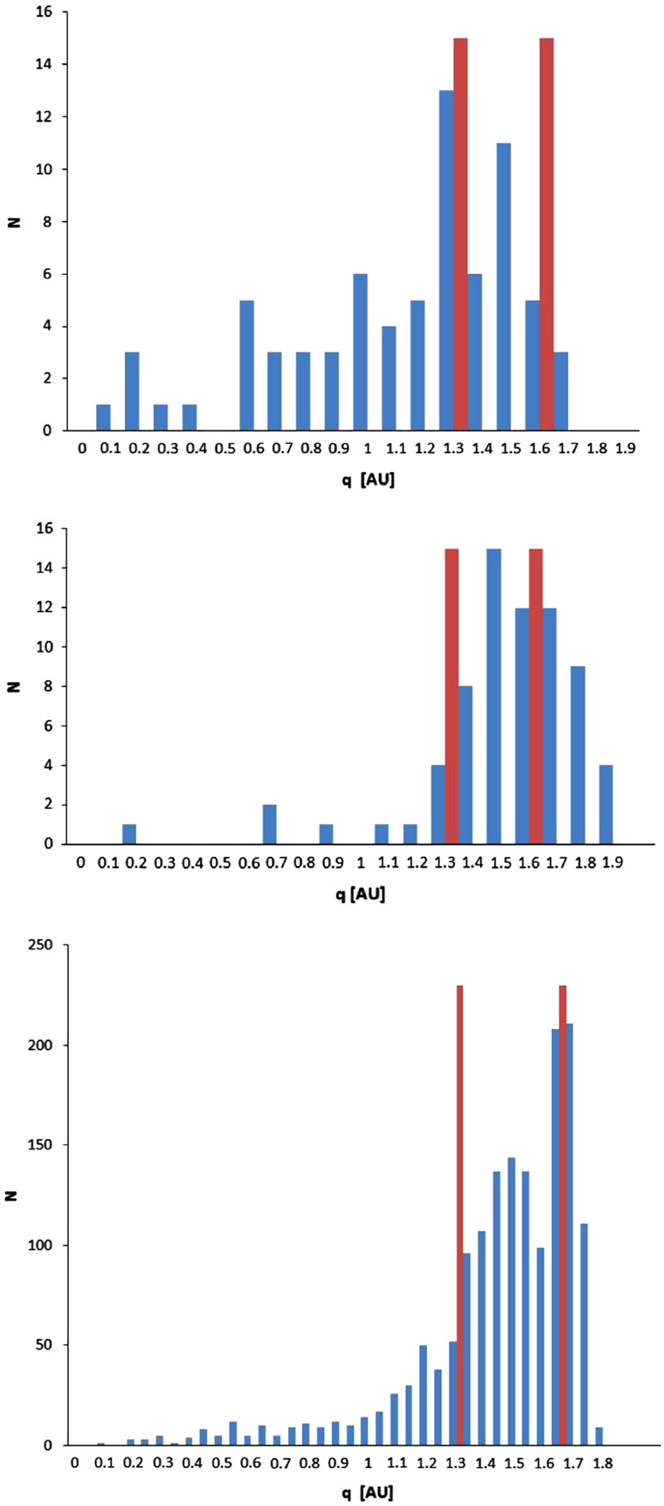

Fig. 2. Perihelion distance distribution for the sample of Long Period comets (top), Jupiter Family comets (middle) and asteroids (bottom) used in constructing the sporadic meteoroid flux model as explained in the text. (For interpretation of the references to colour in the main text the reader is referred to the web version of this article.)

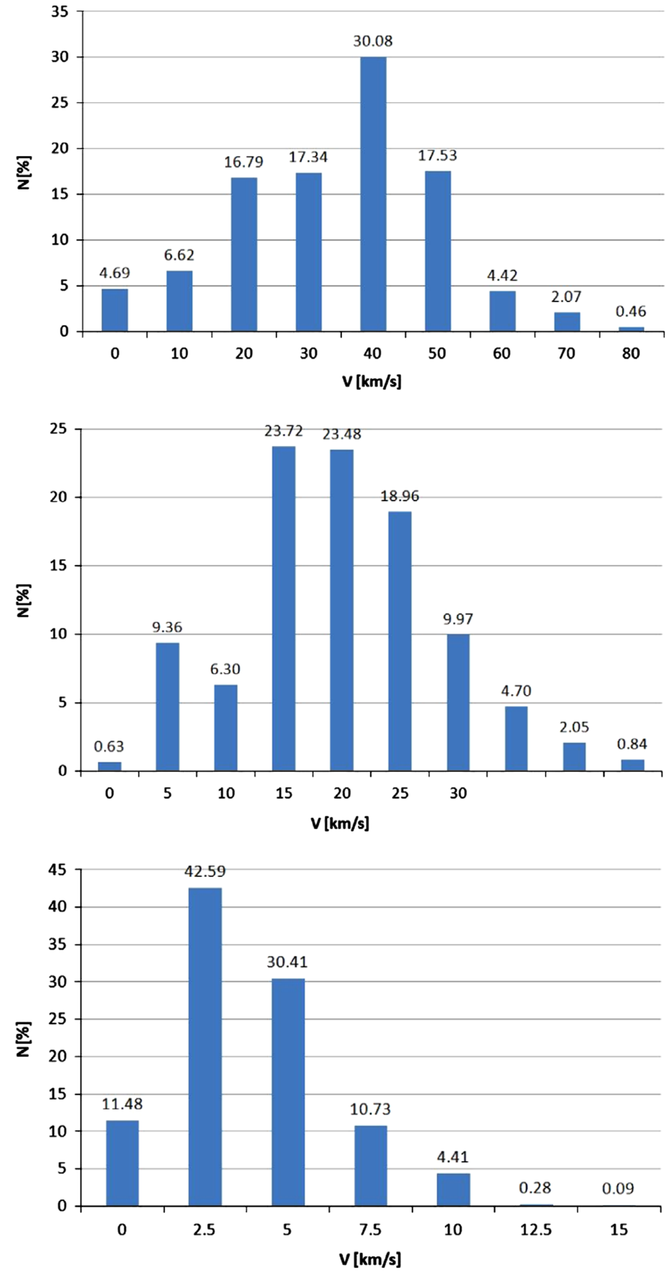

Fig. 3. Impact velocity distribution for the sample of Long Period comets (top), Jupiter Family comets (middle) and asteroids (bottom) used in constructing the sporadic meteoroid flux model as explained in the text.

$g = 2.81$ also used by Gallant et al. when investigating the flux asymmetry on the Earth's Moon.

If we adopt typical v_∞ values for LPC (JFC) impactors of 40 (20) km s^{-1} respectively (assuming $v_\infty \simeq v_{imp}$ if either is much larger than the escape velocity), we obtain relative crater densities (i.e. $\Gamma/\overline{\Gamma}$) of 1.12 (1.24) and 0.89 (0.79) for $\beta = 0^\circ$ and $\beta = 180^\circ$ respectively or apex–antapex differences of 7% and 14% respectively. Adopting $\langle v_\infty \rangle = 4$ km s^{-1} for asteroidal impacts yields values of 2.15 and 0.30, a difference by a factor of ~ 7 between apex and antapex crater density. The statistical output of our model (Table 1) for the Leading and Trailing sectors predicts a difference of 7% for both LPCs and JFCs and a factor of ~ 4 difference for asteroidal impactors.

As can be seen in column 6 of Table 1, the observed crater densities on the leading and trailing sides of Phobos show an asymmetry of a factor of ~ 2 that, if taken at face value, can be interpreted as a vindication of our model for an approximately equal ratio of cometary/asteroidal impacts (actually 43/57). We prefer to treat this result with some caution. Some of the reasons, to be addressed in future work, include: (i) our model does not provide us with a self-consistent steady state, either in the Mars-approaching population of impactors or the production of craters, (ii) consideration of the efficiency of meteoroid delivery from different sources was not done as rigorously as in previous works dealing with the sporadic flux at the Earth, (iii) the observed craters likely formed >1 Gyr ago when Phobos' orbit would have been wider and its orbital velocity lower owing to tidal evolution, (iv) Phobos' shape (including its departure from sphericity) may result in preferential shielding of some areas over others and thus skew the statistics, and (v) the possibility that Phobos broke its rotational lock to Mars when one or more of its craters formed.

Nevertheless, our results demonstrate the potential of models of this type for constraining the relative contributions to the impact flux in the Martian system from different source populations when combined with accurate crater inventories for Phobos that are now available.

7. Conclusions and future prospects

Despite the current intense scientific interest on Mars, direct measurements of its meteoroid environment have not been forthcoming. In terms of Phobos science, it would be important to feed these into models that attempt to reproduce the main features of its crater population as well as predictions of its dust torus. In the foreseeable future, some progress is expected through the ongoing detection campaign of new impact craters caused by large meteoroids on Mars by the HiRISE camera onboard the Mars Reconnaissance Orbiter (Daubar et al., 2011) and the detection of impacts by a seismometer to be placed on Mars in 2016 as part of the InSight mission (Lognonne and InSight SEIS VBB Team, 2012). The possibility and value of coordinated observations has also been recognised (Daubar et al., 2012). The detection of smaller meteoroids, on the other hand, must await the arrival of the first meteor camera in the vicinity of Mars (Christou et al., 2012).

Acknowledgements

This paper has been prepared following the 7th European Strategic Meteor workshop sponsored by the Europlanet Research Infrastructure (RI) and held at the Moscow State University of Geodesy and Cartography in 5–6 July 2012. This work has been supported by Grant 11.G34.31.0021 from the Ministry of Education and Science of the Russian Federation. MG was supported by the Academy of Finland. Astronomical research at the Armagh Observatory is funded by the Northern Ireland Department of Culture, Arts and Leisure (DCAL).

References

Adolfsson, L., Gustafson, B.A.S., Murray, C.D., 1996. The Martian atmosphere as a meteoroid detector. Icarus 119, 144–152.
Archinal, B.A., 15 co-authors, 2009. Division I–III/working group cartographic coordinates and rotational elements. In: Transactions of the IAU 4, p. 68.
Atreya, P., Christou, A.A., 2009. The 2007 Aurigid meteor outburst. Monthly Notices of the Royal Astronomical Society 393, 1493–1497.
Babadzhanov, P.B., 1994. Density of meteoroids and their mass influx on the Earth. In: Milani, A., Di Martino, M., Cellino, A. (Eds.), Proceedings of Asteroids, Comets, Meteors 1993. Kluwer, Dordrecht, pp. 45–54.
Bellot Rubio, L.R., Martínez González, M.J., Ruiz-Herrera, L., Licandro, J., Martínez-Delgado, J., Rodríguez-Gil, M., Serra-Ricart, M., 2002. Modeling the photometric and dynamical behavior of Super-Schmidt meteors in the Earth's atmosphere. Astronomy and Astrophysics 389, 680–691.
Bottke, W.F., Love, S.G., Tytell, D., Glotch, T., 2000. Interpreting the elliptical crater populations on Mars, Venus and the Moon. Icarus 145, 108–121.
Brown, P.J., Weryk, R., Wong, D., Jones, J., 2008. A meteoroid stream survey using the Canadian Meteor Orbit Radar. I. Methodology and radiant catalogue. Icarus 195, 317–339.
Chappelow, J.E., Sharpton, V.L., 2006. Atmospheric variations and meteorite production on Mars. Icarus 184, 424–435.
Chesley, S.R., Chodas, P.W., Milani, A., Valsecchi, G.B., Yeomans, D.K., 2002. Quantifying the risk posed by potential Earth impacts. Icarus 159, 423–432.
Christou, A.A., 2010. Annual meteor showers at Venus and Mars: lessons from the Earth. Monthly Notices of the Royal Astronomical Society 402, 2759–2770.
Christou, A.A., Beurle, K., 1999. Meteoroid streams at Mars: possibilities and implications. Planetary and Space Science 47, 1475–1485.
Christou, A.A., Oberst, J., Elgner, S., Flohrer, J., Margonis, A., McAuliffe, J.P., Koschny, D., 2012. Orbital observations of meteors in the Martian atmosphere using the SPOSH camera. Planetary and Space Science 60, 229–235.
Christou, A.A., Vaubaillon, J., 2011. Numerical modeling of cometary meteoroid streams encountering Mars and Venus. In: Cooke, W.J., Moser, D.E., Hardin, B.F., Janches, J. (Eds.), Meteoroids: The Smallest Solar System Bodies. NASA/CP-2011-216469, pp. 26–30.
Daubar, I.J., McEwen, A.S., Byrne, S., Dundas, C., 2012. Ongoing impact events on Mars: implications for science and exploration. In: Concepts and Approaches for Mars Exploration. LPI Contr. 1679. p. 4301.
Daubar, I.J., McEwen, A.S., Byrne, S., Dundas, C.M., Keska, A.L., Amaya, G.L., Kennedy, M., Robinson, M.S., 2011. New craters on Mars and the Moon. In: Lunar and Planetary Science Conference, The Woodlands, Texas, March 7–11, 2011. LPI Contr. 1608. p. 2232.
Dmitriev, V.M., Lupovka, V.A., Sizenkov, V., Oberst, J., 2012a. Comet population near Mars and predicted meteoroid encounters with Phobos. In: European Planetary Science Congress 2012, EPSC Abstracts Vol. 7, EPSC2012-204.
Dmitriev, V.M., Lupovka, V.A., Sizenkov, V., Oberst, J., 2012b. Simulations of meteoroid impacts on Phobos and global crater distributions. In: European Planetary Science Congress 2012, EPSC Abstracts Vol. 7, EPSC2012-621.
Domokos, A., Bell III, J.F., Lemmon, M.T., Brown, P., Suggs, R., Vaubaillon, J., Cooke, W., 2007. Measurement of the meteoroid flux at Mars. Icarus 191, 141–150.
Farinella, P., Vokrouhlicky, D., Hartmann, W.K., 1998. Meteorite delivery via Yarkovsky orbital drift. Icarus 132, 378–387.
Flynn, G.J., McKay, D.S., 1989. An assessment of the meteoritic contribution to the Martian soil. Journal of Geophysical Research 95, 14497–14509.
Gallant, J.B., Gladman, B.T., Ćuk, M., 2009. Current bombardment of the Earth–Moon system: emphasis on cratering asymmetry. Icarus 202, 371–382.
Grün, E., Zook, H.A., Fechtig, H., Giese, R.H., 1985. Collisional balance of the meteoritic complex. Icarus 62, 244–272.
Hughes, D.W., 1987. P/Halley dust characteristics - A comparison between Orionid and Eta 888. Aquarid meteor observations and those from the flyby spacecraft. Astronomy and Astrophysics 187, 879–888.
Ito, T., Malhotra, R., 2010. Asymmetric impacts of near-Earth asteroids on the Moon. Astronomy and Astrophysics 519, A63.
Ivanov, B.A., Neukum, G., Bottke, W.F.J., Hartmann, W.K., 2002. The comparison of size-frequency distributions of impact craters and asteroids and the planetary cratering rate. In: Bottke, W.F., Cellino, A., Paolicchi, P., Binzel, R.P. (Eds.), Asteroids III. University of Arizona Press, Tucson, pp. 89–101.
Jenniskens, P., 2006. Meteor Showers and Their Parent Comets. Cambridge University Press, Cambridge.
Jones, J., Brown, P., 1993. Sporadic meteor radiant distributions—orbital survey results. Monthly Notices of the Royal Astronomical Society 265, 524–532.
Kawamura, T., Morota, T., Kobayashi, N., Tanaka, S., 2011. Cratering asymmetry on the Moon: a new insight from the Apollo Passive Seismic Experiment. Geophysical Research Letters 38 (May), L15201.
Kharachevtseva, I.P., Zubarev, A.E., Nadezhdina, I.E., Uchaev, D.V., Uchaev, Dm.V., Malinnikov, V.A., Klimkin, N.D., Cherepanova, E.V., Garov, A.S., Oberst, J., 2014. The Phobos Information System. Planetary and Space Science 102, 74–85, http://dx.doi.org/10.1016/j.pss.2013.05.012.
Kikwaya, J.B., Brown, P., Campbell-Brown, M., Nudds, S., 2006. The bulk density of meteoroids from electro-optical measurements. In: Pre-Solar Grains as Astrophysical Tools, Prague, Czech Republic, 21 October 2006.
Krivov, A.V., Hamilton, D.P., 1997. Martian dust belts: waiting for discovery. Icarus 128, 335–353.
Larson, S.L., 2001. Determination of meteor showers on other planets using comet ephemerides. Astronomical Journal 121, 1722–1729.
Le Feuvre, M., Wieczorewk, M.A., 2011. Nonuniform cratering of the Moon and a revised crater chronology of the inner Solar System. Icarus 214, 1–20.
Lebedinets, V.N., 1987. The declaration of faint photographic meteors and the density of meteoroids. Astronomicheskii Vestnik 21, 65–74. (in Russian).
Levin, P.B., 1956. The physical theory of meteors and the study of the space density of meteor matter. Bulletin of the Astronomical Institutes of Czechoslovakia 7, 58–59.
Lognonne, P., InSight SEIS VBB Team, 2012. The insight VBB seismometer: from signal and noise to internal structure. In: European General Assembly 2012, EPSC Abstracts Vol. 14, EGU2012-12945.
McAuliffe, J.P., 2006. Modelling Meteor Phenomena in the Atmospheres of the Terrestrial Planets. Ph.D. Thesis. Queen's University Belfast.
McAuliffe, J.P., Christou, A.A., 2006. Simulating meteor showers in the Martian atmosphere. In: Proceedings of the International Meteor Conference, 15–18 September, 2005. International Meteor Organisation. Oostmalle, Belgium, pp. 155–160.
McIntosh, B.A., 1991. Debris from comets—the evolution of meteor streams. In: Comets in the Post-Halley Era, pp. 557–591.
McNaught, R.H., Asher, D.J., 1999. Leonid dust trails and meteor storms. WGN, Journal of the International Meteor Organization 27, 85–102.
Neslusan, L., 2005. The potential meteoroid streams crossing the orbits of terrestrial planets. Contributions of the Astronomical Observatory Skalnate Pleso 35, 163–179.

Oberst, J., Flohrer, J., Elgner, S., Maue, T., Margonis, A., Schrödter, R., Tost, W., Buhl, M., Ehrich, J., Christou, A., Koschny, D., 2011. The Smart Panoramic Optical Sensor Head (SPOSH)—a camera for observations of transient luminous events on planetary night sides. Planetary and Space Science 59, 1–9.

Oberst, J., Nakamura, Y., 1991. A search for clustering among the meteoroid impacts detected by the Apollo lunar seismic network. Icarus 91, 315–325.

Opik, E.J., 1976. Interplanetary Encounters: Close-Range Gravitational Interactions. Elsevier Scientific Publishing Company, 164p.

Pätzold, M., Tellmann, S., Häusler, B., Hinson, D., Schaa, R., Tyler, G.L., 2005. A sporadic third layer in the ionosphere of Mars. Science 310, 837–839.

Popova, O., Nemtchinov, I., Hartmann, W.K., 2003. Bolides in the present and past martian atmosphere and effects on cratering processes. Meteoritics and Planetary Science 38, 905–925.

Press, W., Teukolsky, S.A., Vetterling, W.T., 2007. Numerical Recipes. The Art of Scientific Computing, 3rd edition Cambridge University press, Cambridge 1237p.

Richardson, J.E., Melosh, H.J., Artemieva, N.A., Pierazzo, E., 2005. Impact cratering theory and modelling for the Deep Impact mission: from mission planning to data analysis. Space Science Reviews 117, 241–267.

Selsis, F., Brillet, J., Rappaport, M., 2004. Meteor showers of cometary origin in the Solar System: revised predictions. Astronomy and Astrophysics 416, 783–789.

Selsis, F., Lemmon, M.T., Vaubaillon, J., Bell, J.F., 2005. Extraterrestrial meteors: a martian meteor and its parent comet. Nature 435, 581.

Terentjeva, A., 1993. Meteor bodies near the orbit of Mars. In: Roggemans, P. (Ed.), Proceedings of IMO Conference, pp. 97–105.

Treiman, A.H., Treiman, J.S., 2000. Cometary dust streams at Mars: preliminary predictions from meteor streams at Earth and from periodic comets. Journal of Geophysical Research 105, 24571–24582.

Wiegert, P., Vaubaillon, J., Campbell-brown, M., 2009. A dynamical model of the sporadic meteoroid complex. Icarus 201, 295–310.

Zahnle, K., Schenk, P., Sobieszczyk, S., Dones, L., Levison, H.F., 2001. Differential cratering of synchronously rotating satellites by ecliptic comets. Icarus 153, 111–129.